PNAS RESEARCH ARTICLE | IMMUNOLOGY AND INFLAMMATION

Chronic stress induces colonic tertiary lymphoid organ formation and protection against secondary injury through IL-23/IL-22 signaling

Adrian Gomez-Nguyen[a,b], Nikhilesh Gupta[a], Harsha Sanaka[a], Dennis Gruszka[a], Alaina Pizarro[a], Luca DiMartino[a,b], Abigail Basson[a,b], Paola Menghini[a,b], Abdullah Osme[a,c], Carlo DeSalvo[c], Theresa Pizarro[a,b,c], and Fabio Cominelli[a,b,c,1]

Edited by Kiyoshi Takeda, Osaka Daigaku, Suita, Japan; received May 11, 2022; accepted August 17, 2022, by Editorial Board Member Tadatsugu Taniguchi

Psychological stress has been previously reported to worsen symptoms of inflammatory bowel disease (IBD). Similarly, intestinal tertiary lymphoid organs (TLOs) are associated with more severe inflammation. While there is active debate about the role of TLOs and stress in IBD pathogenesis, there are no studies investigating TLO formation in the context of psychological stress. Our mouse model of Crohn's disease–like ileitis, the SAMP1/YitFc (SAMP) mouse, was subjected to 56 consecutive days of restraint stress (RS). Stressed mice had significantly increased colonic TLO formation. However, stress did not significantly increase small or large intestinal inflammation in the SAMP mice. Additionally, 16S analysis of the stressed SAMP microbiome revealed no genus-level changes. Fecal microbiome transplantation into germ-free SAMP mice using stool from unstressed and stressed mice replicated the behavioral phenotype seen in donor mice. However, there was no difference in TLO formation between recipient mice. Stress increased the TLO formation cytokines interleukin-23 (IL-23) and IL-22 followed by up-regulation of antimicrobial peptides. SAMP × IL-23r$^{-/-}$ (knockout [KO]) mice subjected to chronic RS did not have increased TLO formation. Furthermore, IL-23, but not IL-22, production was increased in KO mice, and administration of recombinant IL-22 rescued TLO formation. Following secondary colonic insult with dextran sodium sulfate, stressed mice had reduced colitis on both histology and colonoscopy. Our findings demonstrate that psychological stress induces colonic TLOs through intrinsic alterations in IL-23 signaling, not through extrinsic influence from the microbiome. Furthermore, chronic stress is protective against secondary insult from colitis, suggesting that TLOs may function to improve the mucosal barrier.

inflammatory bowel disease | IL-23 | stress | microbiome | Tertiary Lymphoid Organs

Inflammatory bowel disease (IBD) is a chronic relapsing and remitting disorder of the gastrointestinal tract that is further subdivided into two categories: Crohn's disease (CD) and ulcerative colitis (UC). While enormous strides have been made to better understand the pathogenesis of IBD and its etiology, a definitive mechanism has remained elusive (1, 2). Therefore, the need to identify environmental triggers and etiologies remains critical to address unmet therapeutic needs (3). Psychological stress has been repeatedly shown to be a significant risk factor for IBD patients. IBD patients with high perceived stress are more likely to require biologics, corticosteroids, and surgical intervention even if they are currently in remission (4–8). Animal studies investigating the relationship between stress and IBD have largely been performed in models of acute colitis, such as dextran sodium sulfate (DSS) (9, 10). While these models are unequivocally valuable, there remains little work done to investigate the role of stress in chronic models of IBD and small intestinal inflammation. Furthermore, the majority of patients with CD have inflammation in the terminal ileum (11). Therefore, there is a clear need to investigate how chronic ileitis is affected by stress.

In addition to psychological stress, a growing body of work suggests an important role for tertiary lymphoid organs (TLOs) in the disease process of IBD (12, 13). While TLOs have long been recognized to be associated with IBD, there is still debate whether they play a protective or pathogenic role (14, 15). TLOs are formed postnatally and are characterized as densely packed clusters of CD4^{+} T cells, follicular dendritic cells (DCs), and B cells. While the subtleties of the TLO formation pathway are still being investigated, there is general agreement that TLO formation is ultimately dependent on interleukin-23 (IL-23)–mediated up-regulation of CXCL13 (16). Characterization of upstream TLO formation signals is complicated by potential redundancies in the pathway (13). While there is some work that has shown that glucocorticoids

Significance

Here, we demonstrate that chronic stress induces the formation of tertiary lymphoid organs (TLOs) in the colon of a mouse model of Crohn's disease (CD)-like ileitis. Stress induces increased production of interleukin-23 (IL-23) and IL-22, which subsequently increases TLO formation and production of antimicrobial peptides. Interestingly, chronic stress is also protective against chemically induced colitis. While previous studies have linked stress and glucocorticoids to constituents of the TLO formation pathway, our study shows that stress directly increases TLO formation. Furthermore, stress is canonically associated with more severe inflammation. However, not all patients who experience stress have worse disease. Therefore, this study has translational significance because it demonstrates a condition where stress has a beneficial effect.

Author contributions: A.G.-N., T.P., and F.C. designed research; A.G.-N., N.G., H.S., D.G., A.P., L.D., A.B., P.M., A.O., and C.D. performed research; A.G.-N., D.G., A.B., P.M., A.O., T.P., and F.C. analyzed data; and A.G.-N. and F.C. wrote the paper.

The authors declare no competing interest.

This article is a PNAS Direct Submission. K.T. is a guest editor invited by the Editorial Board.

[1]To whom correspondence may be addressed. Email: fabio.cominelli@uhhospitals.org.

This article contains supporting information online at http://www.pnas.org/lookup/suppl/doi:10.1073/pnas.2208160119/-/DCSupplemental.

Published September 26, 2022.

can alter components of the TLO formation pathway, there have been no data showing that psychological stress can impact TLO formation (17–20).

Here, we performed restraint stress (RS) to induce chronic psychological stress on our mouse model of CD-like ileitis, the SAMP1/YitFc (SAMP) mouse. The SAMP mouse develops spontaneous and persistent CD-like ileitis, but not colitis, without external manipulation (21). We have previously shown that, despite profound intestinal inflammation, the SAMP mouse does not exhibit locomotor deficits, depressive-like behavior, or anxiety-like behavior at baseline (22). Stressed mice did not develop colitis or have worse ileitis. Despite not normally exhibiting colonic inflammation, stressed SAMP mice significantly increased the number of colonic TLOs. Stress did not alter the genus-level composition of the microbiome. While fecal microbiome transplantation (FMT) of stool from stressed SAMP mice to germ-free (GF) mice did replicate behavior, there was no difference in the number of TLOs compared to mice transplanted with unstressed (US) stool. We found that stressed mice up-regulated TLO formation pathway constituents, and SAMP × IL23r$^{-/-}$ mice did not have increased TLOs following stress. Finally, we show that stress is protective against secondary injury from DSS-induced colitis by a mechanism involving up-regulation of IL-22 and antimicrobial peptides (AMPs).

Results

Stressed Mice Have Increased Formation of TLOs. Previous work has demonstrated that while SAMP mice predictably develop ileitis by 10 wk, they do not develop colitis (21). Furthermore, we have shown that despite profound ileitis, SAMP mice do not exhibit spontaneous behavioral abnormalities (22). We therefore reasoned that the SAMP mouse would make an ideal model to investigate the relationship between chronic induced stress and intestinal inflammation. We utilized RS, a well-recognized model of stress, to induce chronic stress on 12-wk–old SAMP mice for 56 consecutive days (23, 24).

Using three-dimensional (3D) stereomicroscopy, we found a dramatic increase in the number of structures that resembled TLOs in RS-SAMP mice compared to in US control mice (Fig. 1*A*) (25). The presumptive TLOs were ∼1 mm in diameter and were found more frequently in the distal colon. Hematoxylin and eosin (H&E) staining of the growths revealed a high-density lymphocyte environment with the presence of plasma cells (Fig. 1*B*). To characterize the cell population in the TLOs, we used the GeoMx digital spatial profiler from NanoString and performed whole-transcriptome analysis of the TLOs. We then performed deconvolution using the SpatialDecon R library to determine immune cell abundance (26). As predicted, B cells were found to be the dominant immune cell type within the TLOs. Innate lymphoid cells (ILCs), particularly ILC3s, T cells, and antigen-presenting cells, were also highly represented (Fig. 1*C*). Although RS-SAMP mice exhibited a dramatic increase in colonic TLOs, the composition of the TLOs was largely unchanged compared to US-SAMP mice. Flow cytometric analysis of isolated TLOs revealed that levels of B cells, macrophages, DCs, and both CD4$^+$ and CD8$^+$ T cells were similar between US-SAMP and RS-SAMP mice (Fig. 1*D*).

Chronic Psychological Stress Alters Behavior but Not Intestinal Inflammation in SAMP Mice. Compared to US mice, SAMP mice subjected to RS exhibited some decrease in anxiety-like behavior during the elevated plus maze (EPM) (Fig. 2*A*). However, this result was not replicated in the open field (OF) test, another assay of anxiety-like behavior (Fig. 2*B*). SAMP mice exhibited a profound increase in immobility times during tail suspension (TS), indicating a depressive-like phenotype (Fig. 2*C*). Other measures of behavior were not significantly altered compared to the US group (*SI Appendix*, Fig. S1 A–C). Contrary to our original hypothesis, histopathologic assessment of RS-SAMP mice did not demonstrate more severe ileitis nor was there evidence of colitis (Fig. 2*D*). The histopathologic findings were reflected by no significant differences in immune cell profiles of the mesenteric lymph node (MLN) (Fig. 2*E*). T cell cytokine production was similarly unchanged between stressed and US-SAMP mice (*SI Appendix*, Fig. S2 A and B). Collectively, these results demonstrate that while the SAMP mouse is susceptible to stress, there does not seem to be an effect on intestinal inflammation, and, critically, increased formation of TLOs is not a result of colitis or more severe ileitis. These findings lead us to hypothesize that stress promotes TLO formation through either extrinsic (i.e., microbiome alterations) or intrinsic (i.e., glucocorticoid signaling) factors.

The Microbiome from Stressed Mice Is Altered but Does Not Induce TLO Formation. The microbiome has been repeatedly implicated in the disease process of IBD and other intestinal disorders (27). The bidirectional microbiome–gut axis, in particular, is the subject of intense investigation (28, 29). Given the mutability of the gut microbiome and the body of evidence for the microbiome–gut–brain axis, we reasoned that stress could exert its influence through alterations in the gut microbiome. However, 16S ribosomal RNA (rRNA) analysis of the gut microbiome from RS-SAMP and US-SAMP mice revealed no persistently significant differences in microbiome composition (Fig. 3*A*). While there were no compositional changes revealed in our analysis, 16S rRNA analysis provides only genus-level resolution; it is not capable of reliable species-level analysis. Furthermore, metabolic and functional changes to existing taxa are outside the scope of 16S rRNA analysis. Given the inherent shortcomings of 16S rRNA analysis, we could not discount the possibility that the microbiome was altered in the RS-SAMP mice, and, therefore, we could not discount the hypothesis that stress promotes TLO formation through microbiome alterations.

To investigate our hypothesis more completely, we harvested stool from US-SAMP and RS-SAMP donors. We then performed an FMT of the donor stool into GF US-SAMP mice. FMT was performed using oral gavage instead of cohousing to ensure that there was no bias toward aerobic bacteria (30). In-line with other work investigating transference of behavior following FMT, recipient mice replicated the depressive-like behavior seen in the RS-SAMP donor mice (*SI Appendix*, Fig. S3*A*) (31). Interestingly, FMT from RS-SAMP donors also developed anxiety-like behavior on both EPM and OF tests (*SI Appendix*, Fig. S3*B*). Other measures of behavior were unchanged in recipient mice (*SI Appendix*, Fig. S3 *D–F*). The microbiome of recipient mice remained largely similar at all time points (*SI Appendix*, Fig. S3*G*). Despite replicating the behavioral phenotype, FMT from RS-SAMP mice did not induce greater TLO formation than FMT from US-SAMP mice (Fig. 3*B*). Similarly, immune cell composition of colonic TLOs was unchanged, with the exception of DCs, which were increased in RS-SAMP recipients (Fig. 3*C*).

Altogether, our findings suggest that while chronic stress induces functional changes in the gut microbiome, differential TLO formation does not seem to be dependent on the altered

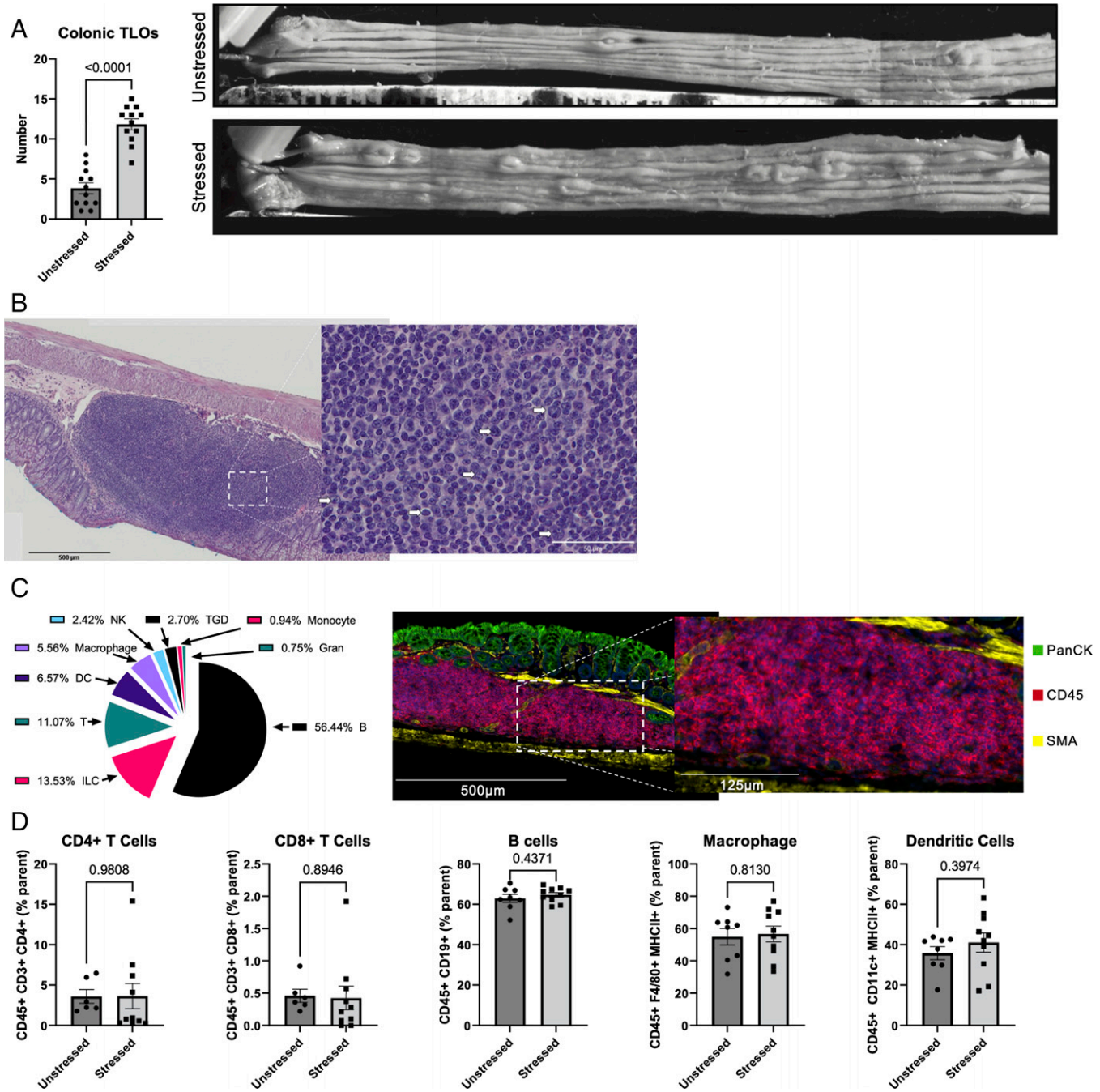

Fig. 1. Stress increases formation of TLOs. (*A*) Representative composite images from stereomicroscopy of the colon with TLO quantification. (*B*) Representative H&E stain of a TLO at ×20 magnification (*Left*) and ×40 magnification (Scale bars, 500 μm and 50 μm) *Right*; white arrows identify potential plasma cells). (*C*) Representative image from the GeoMx digital spatial profiling platform with immune cell deconvolution; TGD, γδ T cell; Gran, granulocyte; NK, natural killer. (Scale bars, 500 μm and 125 μm). (*D*) Flow cytometric analysis of $CD4^+$ T cells, $CD8^+$ T cells, B cells, DCs, and macrophages in TLOs. Data from restrained sex-matched SAMP1/YitFc mice (stressed) compared to unrestrained (US) control mice are shown. Data are presented as mean ± SEM. Exact *P* values from unpaired two-tailed *t* tests are reported, with *P* values <0.05 considered statistically significant.

microbiome. Despite a negative result regarding TLO formation, the findings of this FMT experiment should not be understated. There are clearly differences, be they functional or compositional, that are not appreciated by 16S sequencing alone. FMT provides an efficient and economical supplemental method to assay function and composition.

Stress Increases Production of TLO Formation Pathway Constituents. As the stress-altered microbiome did not explain altered formation of TLOs, we next investigated how stress could affect intrinsic factors. Using GeoMx spatial transcriptomics, we investigated which transcripts were up-regulated in the TLOs of RS-SAMP mice. Several transcripts associated with the TLO formation pathway, B cell recruitment, and plasma cell function were found to be up-regulated in the RS-SAMP mice (Fig. 4*A*). Most notably, we found that transcription of lymphotoxin beta receptor (*ltbr*), *il23a*, and *il22*—key upstream regulators—was increased. In the TLO formation pathway, production of IL-23 is dependent on the interaction of $LT\alpha_1\beta_2$ with its receptor LTβR (32, 33). We confirmed the increased production of IL-23a and IL-22 by enzyme-linked immunosorbent assay (ELISA) of MLN cell culture supernatant and qRT-PCR of LTβR from colonic

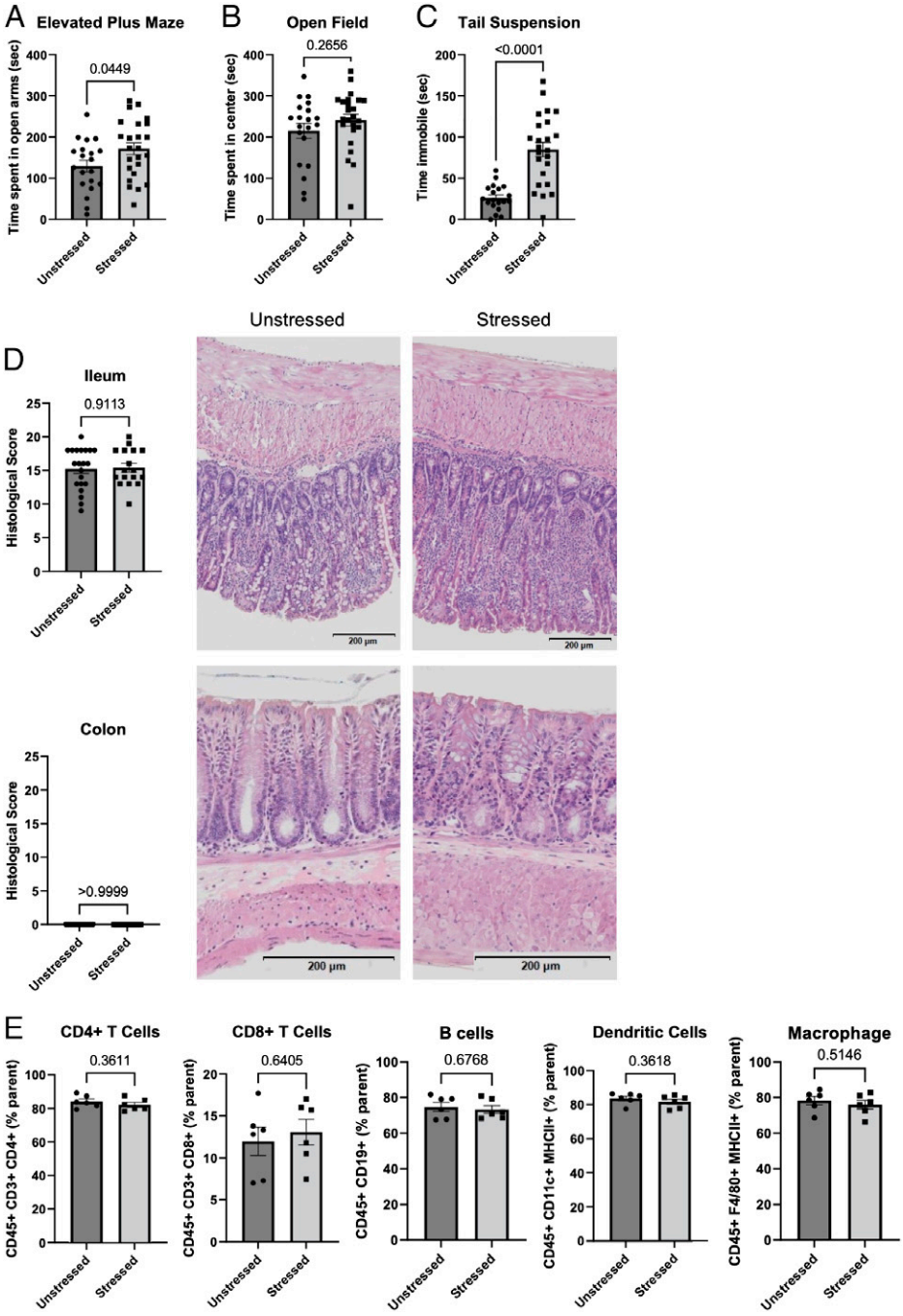

Fig. 2. Chronic psychological stress alters behavior but does not worsen intestinal inflammation. (*A*) Time spent in open arms of the EPM after 56 d of RS. (*B*) Time spent in the center of the OF test. (*C*) Time immobile during the TS test. (*D*) Representative H&E staining of ileum (*Top*) and colon (*Bottom*) with pathological score. (Scale bar, 200 µm). (*E*) Flow cytometric analysis of $CD4^+$ T cells, $CD8^+$ T cells, B cells, DCs, and macrophages in MLNs. Data are from restrained sex-matched SAMP1/YitFc mice (stressed) compared to unrestrained (US) control mice. Data are representative of three independent experiments and are presented as mean ± SEM. Exact *P* values from Mann–Whitney or unpaired two-tailed *t* tests are reported, and *P* values <0.05 were considered statistically significant.

tissue (Fig. 4 *B* and *C*). Production of several AMPs, a recognized downstream product of IL-22 signaling, was also significantly increased in the RS-SAMP mice (Fig. 4*D*) (34, 35).

To further interrogate the mechanism, we generated SAMP × $IL23r^{-/-}$ ($IL23r^{-/-}$) mice with a nonfunctional IL-23 receptor (36). We then administered intraperitoneal (i.p.) recombinant IL-22 (rIL22) to a group of $IL23r^{-/-}$ mice. This resulted in four groups of $IL23r^{-/-}$ mice: US + sham (US-$IL23r^{-/-}$), stressed + sham (RS-$IL23r^{-/-}$), US + rIL22 (US-rIL22 + $IL23r^{-/-}$), and stressed + rIL22 (RS-rIL22 + $IL23r^{-/-}$). IL-23 was identified as a candidate because previous work has demonstrated several redundancies in the TLO formation pathway upstream of the IL-23 receptor (37, 38). Conversely, IL-22, a downstream product of IL-23 signaling, has been shown to be necessary and sufficient to induce TLO formation (32, 39).

RS-$IL23r^{-/-}$ mice did not have increased formation of TLOs compared to US-$IL23r^{-/-}$ mice (Fig. 4*E*). However, TLO formation was rescued by administration of rIL22 in both US-rIL22 + $IL23r^{-/-}$ and RS-rIL22 + $IL23r^{-/-}$ mice (Fig. 4*E*). As expected, while production of IL-23 was increased in the RS-IL-$23r^{-/-}$ mice, IL-22 production was not altered between US and RS groups (Fig. 4*F*). This confirms our

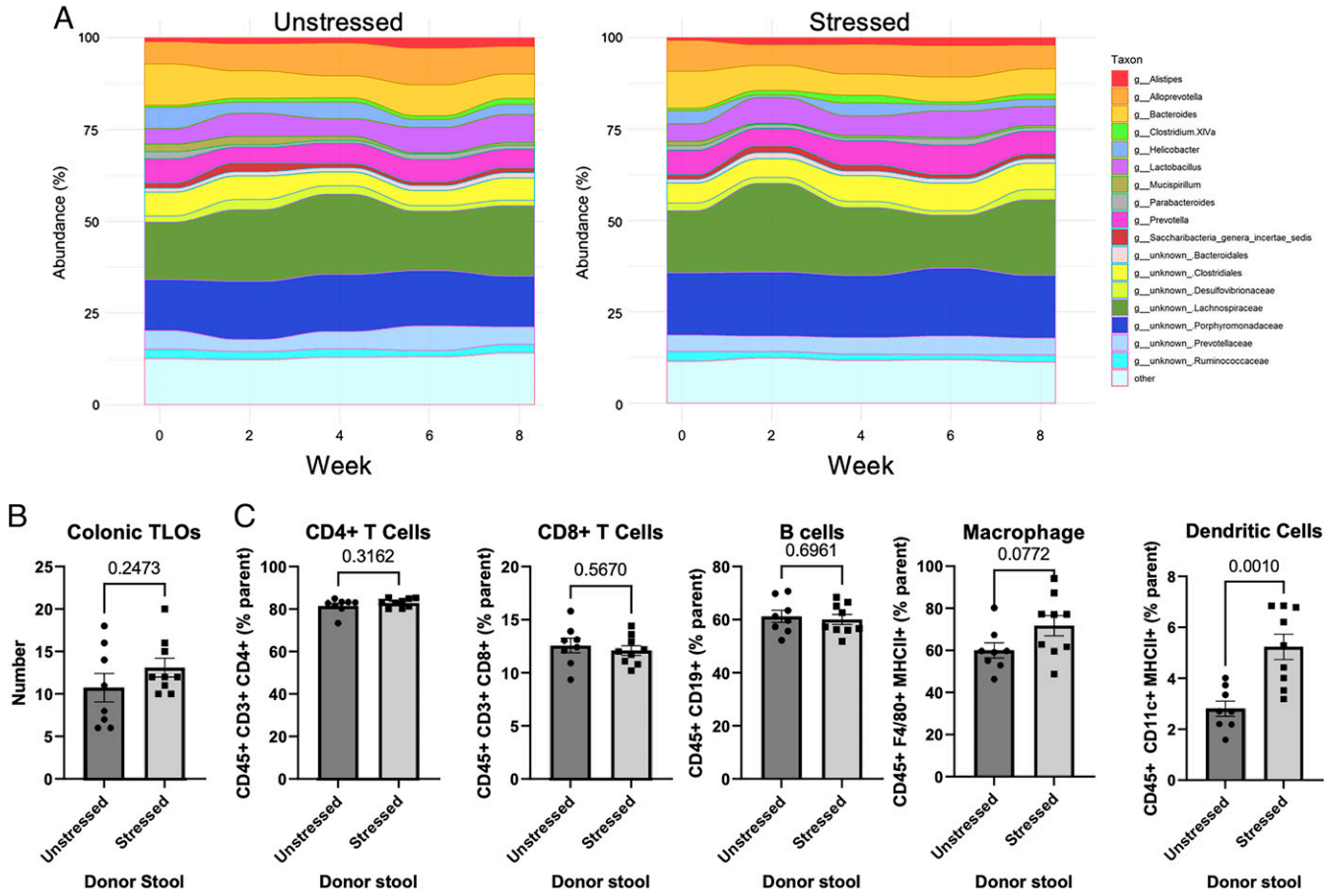

Fig. 3. The microbiome from stressed mice is altered but does not alter TLO formation. (*A*) Alluvial plots showing relative abundance of bacterial genera from US (*Left*) and stressed (*Right*) mice. (*B*) Quantification of colonic TLOs following FMT from US and stressed donors to US GF recipients. (*C*) Flow cytometric analysis of $CD4^+$ T cells, $CD8^+$ T cells, B cells, DCs, and macrophages in TLOs of recipient mice. Stool from restrained sex-matched SAMP1/YitFc mice (stressed) or unrestrained (US) control donors was transplanted to US sex-matched GF SAMP1/YitFc mice and compared. Data are presented as mean ± SEM. Exact *P* values from unpaired two-tailed *t* tests are reported, with *P* values <0.05 considered statistically significant.

hypothesis that stress induces TLO formation by increasing production of IL-23 and that IL-22 is sufficient to rescue TLO formation.

Additionally, composition of TLOs did not differ significantly between US-$IL23r^{-/-}$ and RS-$IL23r^{-/-}$ mice (*SI Appendix*, Fig. S4*A*). However, when comparing the TLO composition between wild-type–SAMP and $IL23r^{-/-}$ mice, we found that there was a significant shift. $IL23r^{-/-}$ TLOs had significantly more $CD4^+$ T cells and macrophages (*SI Appendix*, Fig. S5 *A* and *B*). $IL23r^{-/-}$ TLOs also had significantly fewer DCs in addition to a trend of decreased B cells that did not reach statistical significance (*SI Appendix*, Fig. S5 *A* and *B*). Composition of the TLOs in the $IL23r^{-/-}$ mice could be explained as a resultant increase in upstream regulators due to the curtailed downstream signaling proteins.

Chronic Stress Is Protective against Secondary Colonic Injury. Based on previous work that showed an association between TLO formation and worse disease states, RS-SAMP mice were given DSS to induce a secondary colonic insult (12, 40). SAMP mice were stressed, as before, and subsequently administered a 7-d regimen of 3% DSS in their drinking water (days 1 to 7). US-SAMP mice given DSS were used as a control. Interestingly on days 8 and 21, RS-SAMP mice had markedly less severe colitis as observed by endoscopy (Fig. 5*A*). The less severe colitis was also reflected in their histological scores (Fig. 5*B*). Ileitis and body weight were unaffected by administration of DSS (*SI Appendix*, Fig. S6 *A*–*C*). Mice administered DSS did have increased $CD8^+$ T cells and DCs and decreased $CD4^+$ T cell profiles compared to non-DSS controls in MLNs. However, there was no significant difference between US and RS mice in MLN immune cell profiles (Fig. 5*C*). Together, these findings demonstrate that in the context of CD-like ileitis, chronic stress may have protective functions.

Discussion

Here, we have demonstrated that chronic stress induces colonic TLO formation in a mouse model of CD-like ileitis. We found that the increased TLO formation was due to intrinsic alterations to the TLO formation pathway, chiefly, increased IL-23 and IL-22 production. Expression of AMPs (downstream products of IL-22 signaling) was also increased. Interestingly, the increased formation was not due to alterations in the gut microbiome. Additionally, we have demonstrated that, in this model, chronic stress was protective against secondary colonic injury. While there have been innumerable important investigations studying the relationship of stress and IBD, we believe that this study adds a unique viewpoint to the field. The vast majority of murine studies investigating stress and IBD have been performed in models of acute colitis. This is, in part, due to the abundance of colitis models and the relative paucity of ileitis models (41). While many CD patients do have colitis, the ileum is the most commonly affected portion of the

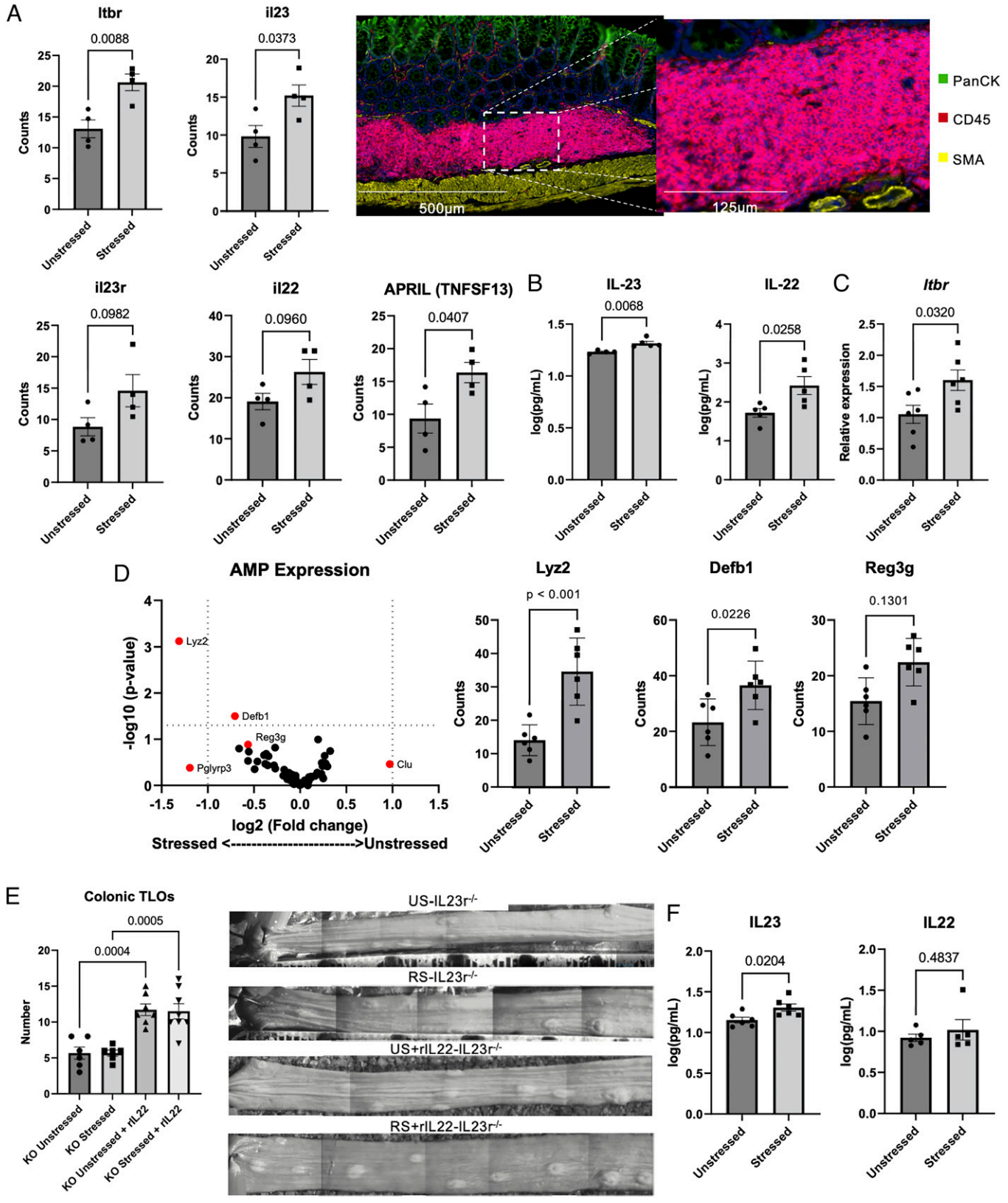

Fig. 4. Stress increases production of TLO formation pathway constituents. (*A*) Representative image of a TLO from GeoMx spatial transcriptomic analysis with probe counts from selected smooth muscle actin (SMA)-negative regions of interest. (Scale bars, 500 μm and 125 μm). (*B*) Concentrations from ELISAs of cell culture supernatant IL-23 (*Left*) and IL-22 (*Right*) in wild-type SAMP1/YitFc mice. (*C*) qRT-PCR measurement of *Itβr* expression from colonic TLOs. (*D*) GeoMx analysis of AMP expression with representative bar graphs. (*E*) Quantification and representative images of colonic TLOs from US or stressed SAMP1/YitFc × IL23r$^{-/-}$ (KO) mice receiving i.p. sham or rIL-22 injection. (*F*) Concentrations from ELISAs of cell culture supernatant IL-23 (*Left*) and IL-22 (*Right*) in restrained (stressed) or unrestrained (US) sex-matched SAMP1/YitFc × IL23r$^{-/-}$ (KO) mice. Data are presented as mean ± SEM. Exact *P* values from unpaired two-tailed *t* tests and ordinary one-way ANOVA are reported, with *P* values <0.05 considered statistically significant. qRT-PCR data are represented as relative expression normalized to *gusb* using the $2^{-\Delta\Delta CT}$ method.

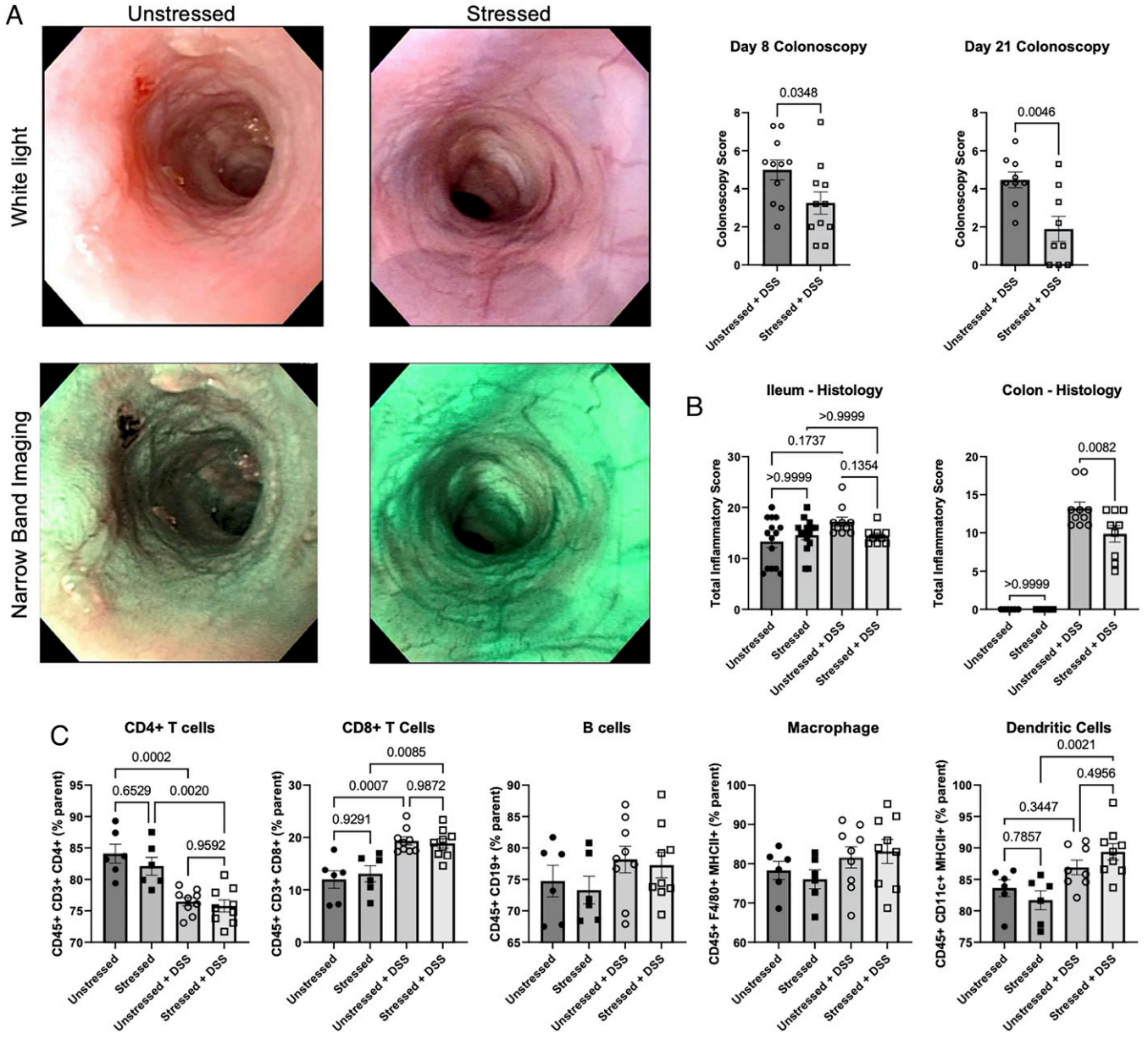

Fig. 5. Chronic stress is protective against secondary colonic insult. (*A*) Colonoscopy scores from day 8 after DSS induction (*Left*) and day 21 after DSS induction (*Right*). Representative images from US (*Left*) and stressed (*Right*) SAMP1/YitFc mice using white light (*Top*) and narrow band imaging (*Bottom*). (*B*) Histological scores from ileum (*Left*) and colon (*Right*). (*C*) Flow cytometric analysis of $CD4^+$ T cells, $CD8^+$ T cells, B cells, DCs, and macrophages in MLNs of mice before and after DSS. Restrained sex-matched SAMP1/YitFc mice (stressed) compared to unrestrained (US) control mice were administered DSS or sham in drinking water. Data are presented as mean ± SEM. Exact *P* values from ordinary one-way ANOVA are reported, with *P* values <0.05 considered statistically significant.

intestinal tract (11, 42). It follows that the response to stress would also be different in UC and CD patients (43). Furthermore, while most studies of IBD patients identify stress as a risk factor for IBD patients, less focus is afforded to IBD patients who are not negatively affected by stress. Therefore, we believe that this study addresses two unanswered questions: how does stress affect a mouse model of ileitis and are there conditions where stress does not increase intestinal inflammation?

The roles of TLOs and their impact on the immune system have been the subject of intense investigation across a wide array of organ systems. The association of IBD and TLOs in particular has been recognized for decades (15). TLOs are formed subsequent to lymphoid tissue inducer (LTi) cell expression of $LT\alpha_1\beta_2$, which binds to LTβR on $CD11c^+$ DCs. This results in the production of IL-23, which induces IL-22 production from T helper 17 (T_h17) cells, ILC3s, and γδ-T cells (32, 33). While there is a well-established formation pathway for TLOs, alterations and modifications to the pathway are still being elucidated. Of particular relevance to the current study, it has been demonstrated that the vagus nerve is capable of inducing colonic TLOs (44). In addition, several studies have illustrated how glucocorticoids may interact with the TLO formation pathway. Separate studies have demonstrated that IL-23 can up-regulate glucocorticoid receptors, glucocorticoids can increase transcriptional activity of LTβR, and a population of IL-22–secreting T_h17 cells are refractory to glucocorticoids (17, 18, 38). While these alterations may normally be innocuous, our study demonstrates how chronic stress, and the resultant disruptions to the hypothalamic–pituitary–adrenal axis, could capitalize on these modifications to induce TLO formation. Administration of rIL22 in our mutant mice did induce TLO formation, as has

been previously demonstrated in non-IBD models (32, 39). Importantly, this demonstrates that while stress significantly alters upstream components of the TLO formation pathway, there does not seem to be significant alterations downstream of IL-22. Given the documented ability of the vagus nerve to influence TLO formation, further work investigating stress in the context of intestinal vagotomy would be valuable.

The microbiome–gut–brain axis has been repeatedly implicated in a variety of disease processes. The microbiome has also been implicated in the formation of TLOs through direct influence on IL-23 and IL-22 production (45, 46). The primary method to analyze microbiome composition, 16S rRNA gene sequencing, has fundamental limitations that must be acknowledged. While there are exciting efforts to improve species- and strain-level identification, genus-level identification remains the most validated and reliable resolution available with 16S analyses (47). In addition, functional differences, which are not assessed with 16S analysis, are being increasingly recognized as an important aspect of the gut microbiome (48, 49). The rationale of our FMT model was based on these two limitations. While we believe the FMT more sufficiently interrogates the influence of the microbiome on TLO formation, it does not completely rule the microbiome out. For example, the possibility still exists that stress induces transient alterations to gut microbiome function, and, after transfer to a US host, the altered function would revert.

While there are some studies that recognize the benefits of stress, they are the considerable minority in the literature (50, 51). In our study, we found that stressed mice had significantly improved acute colitis compared to US mice. Unlike many other models of murine IBD, the SAMP mouse develops inflammation without administration of chemicals, such as DSS. Furthermore, the SAMP mouse has several genetic loci of susceptibility; intestinal inflammation is not due to a specific genetic defect, which is more representative of human disease (21). It is also becoming increasingly apparent that IBD cannot be approached as a monolith. The advent of more sophisticated omics techniques has heralded the notion that specificity beyond the canonical CD and UC subtypes is necessary (52–54). While stress may worsen disease in the majority of IBD patients, the possibility remains that there are patients who may have disease unaffected or improved by stress. Consistent with our findings, recent studies have shown that a moderate amount of stress can improve neurological functions, including oligodendrogenesis (50, 51).

The protective effect of stress in our model could also be explained by the increased IL-22 signaling. IL-22 is known to induce production of AMPs, which are regulators of luminal microbes (34, 35). While the exact mechanism of DSS-induced colitis is not known, it is widely accepted that administration of DSS compromises the mucosal barrier and increases interaction between luminal contents and the mucosal immune system (55). In stressed SAMP mice, the microbiome may be altered as a result of IL-22–mediated AMP production (56). The decreased inflammation in stressed SAMP mice administered DSS may be explained by mitigation of the microbiome by AMPs.

In conclusion, our findings demonstrate that chronic psychological stress increases formation of colonic TLOs in a mouse model of CD-like ileitis. Stress does not appear to induce significant microbiome alterations. Instead, we observed modifications to constituents of the TLO formation pathway, including IL-23 and IL-22. Finally, in this model, we found that chronic stress was protective against secondary colonic injury. Further studies are needed to better understand the dichotomous nature of stress in patients with IBD.

Materials and Methods

Mice. Age- and sex-matched SAMP1/YitFc littermates were obtained from the Mouse Models Core of the National Institutes of Health P30 Digestive Disease Research Core Center. All mice were between 10 and 20 wk of age. SAMP1/YitFc were developed from AKR/J mice through phenotype-guided selective breeding (21). IL23r$^{-/-}$ mice were obtained from Dr. Mohamed Oukka and crossed with the SAMP1/YitFc mouse in the previously mentioned Mouse Models Core (36). All mice were maintained under specific pathogen-free conditions, fed standard chow (Harlan Teklad), and housed in a 12-h light/12-h dark–cycle environment. All procedures were performed after approval by the Institutional Animal Care and Use Committee (protocol number 2014-0158) at Case Western Reserve University (CWRU) and in accordance with American Association for Laboratory Animal Care guidelines.

Histology. Ilea and colons from all mice were removed and flushed with sterile phosphate-buffered saline (PBS; Thermo Fisher) to remove fecal contents. Intestinal tissue was then opened longitudinally and fixed in either Bouin's solution or 10% buffered formalin (Sigma-Aldrich). Samples were stored in fixative for 24 h at 4 °C and washed with 70% ethanol (Thermo Fisher). Tissues were embedded in paraffin and stained with H&E or processed for GeoMx analysis. Intestinal inflammation was scored by a blinded pathologist as previously described (57). Briefly, tissues were assessed on the following three criteria: 1) active inflammation, 2) chronic inflammation, and 3) villus architecture. Each criterion was scored on a scale from 0 to 3, with 0 indicating normal tissue and 1 to 3 representing increasing levels of inflammation. Presence or absence of granuloma, multinucleated histiocytic giant cells, and hypertrophy of the intestinal muscular layer were also noted.

RS. Mice were placed in well-ventilated 50-mL conical tubes for 3 h daily during the procedure. RS occurred over 56 consecutive days. Mice were examined periodically to monitor for injuries.

Behavioral Testing. Mouse behavior was tested in the CWRU Mouse Behavioral Phenotyping Core. Before testing, mice were given 30 min to habituate to the environment. Tests were performed in the following order: OF, EPM, Y-maze (YM), rotarod (RR), and TS. One test per day was performed, and testing was initiated at the same time each day. When applicable, mice were recorded and scored using automated tracking software (ANY-maze). Equipment was cleaned with 10% ethanol between animals. Animals were deidentified before testing to reduce bias. For the OF test, mice were placed in an opaque 50 × 50 cm enclosure for 10 min. The total time spent in the inner area, defined as 7.5 cm from the edge, in addition to total inner area entries were recorded and used to determine anxiety-like behavior and general motor activity, respectfully. For the EPM, mice were placed in a testing apparatus that contained two "closed" arms with opaque walls and two "open" arms. Animals were placed in the same arm to begin the test and were left in the apparatus for 5 min. Time in open arms versus in closed arms was used to assess anxiety-like behavior. For the YM, mice were placed in an apparatus containing three enclosed arms equidistantly spaced 120° apart. Mice were allowed 8 min, and entries into distinct arms were measured to assess short-term spatial memory. For the RR test, mice were placed on a 3-cm rotating dowel (Columbus Instruments). Mice were given 30 s to acclimate to the rod without rotation. This period was followed by a 60-s training period at the lowest rotation speed. Following training, the mice were placed on the rotating dowel with constant acceleration from 4 rpm to 40 rpm (0.1 rpm/s). Mice were given three trials, and the longest "time to fall" was recorded as a measure of motor coordination. For the TS test, mice were suspended from the tip of the tail to a horizontal beam for 6 min. Total immobility time was recorded as a measure of depression-like activity. Immobility time was defined as the absence of escape-like behavior, which includes shaking of the body, movement of the limbs as if running, and attempts to reach the wall or suspension bar. Residual swinging caused by escape-like behavior, without concurrent escape-like behavior, was not classified as immobility. Subtle movements of the forelimbs without accompanying movement from the hindlimbs and vice versa was also not classified as immobility. Strains tested here were not "tail-climbers" and, as such, did not necessitate those precautions.

DSS-Induced Colitis. Induction of colitis was achieved by exposing mice to sterilized 3% (weight/volume) DSS (TdB Consultancy) in drinking water for 7 d and then given normal drinking water for 14 d. To minimize contamination risk, DSS drinking water was renewed every 3 d. Mice were given ad libitum access to water. Monitoring of body weight, bleeding, loose stools, and overall appearance was performed daily.

Colonoscopy. A flexible digital ureteroscope (URF-V), with an 8.5-French (2.8-mm) tapered-tip design, and motion range was used to perform mouse colonoscopies. The endoscope system included a video system center (Olympus America), a xenon light source (Olympus America), and a video recorder (MediCapture). Colonoscopies were performed on days 8 and 21 after DSS administration, and inflammation was evaluated using a previously validated scoring system (58). Mice were anesthetized by isoflurane United States Pharmacopeia USP (Butler Schein Animal Health) before performing an endoscopy. No colonoscopy preparations, such as fasting or laxatives, were required.

FMT. Two wk before stress, fecal samples from all mice were collected and homogenized with 1.0-mm sterilized glass silica beads (BioSpec Products) in PBS with 7% dimethyl sulfoxide. The homogenate was passed through sterile gauze to remove large particulates and to prevent blockage of the gavage needle. FMT with the homogenized stool was then administered to GF and non-GF mice via oral gavage (10 mL/kg) three times in 1 wk to establish a consistent baseline microbiome. Following initiation of stress, feces from stressed and US donor mice was collected and homogenized separately. Recipient mice were administered FMT weekly via oral gavage to mimic the evolution of the microbiome from stress. Oral gavage was chosen over cohousing to prevent artificial selection of obligate aerobes over anaerobes (30).

16S rRNA Gene Microbiome Sequencing and Analysis. DNA purified from snap-frozen stool samples using the QIamp DNA mini kit (Qiagen) was submitted to the CWRU Genomics Core. The core performed quantity (Qubit) and quality (agarose gel electrophoresis) assessments on all submitted samples. The two-step PCR process first used primers to amplify the V3 and V4 regions of the 16S rRNA gene with overhang adapters attached. The second PCR attached unique dual indices and Illumina sequencing adapters using the Nextera XT index kit. Final libraries were quality checked using a Qubit fluorometer to assess concentration and run on agarose gels to verify the correct fragment size (630 base pairs). Libraries were pooled in equimolar volumes and quantified using the NEBNext Illumina library quant kit and Life Technologies Quant Studio 7 real-time PCR system. The pool was diluted and denatured for sequencing using Illumina standard protocols. High-throughput sequencing was performed using an Illumina MiSeq v3 paired-end flowcell. Demultiplexed FASTQ input files were processed using the IMNGS and Rhea bioinformatics pipelines (59, 60). Alluvial plots were generated using the ggalluvial R package.

Cell Isolation and Flow Cytometry. MLNs were aseptically excised immediately following euthanasia per IACUC protocol number 2014-0158 and trimmed of adjacent tissue. TLOs were identified with a stereoscopic microscope and excised with a 1-mm punch biopsy to minimize collection of surrounding tissue. Tissues were gently washed and dispersed through a 40-μm cell strainer in RPMI 1640 complete medium (Gibco) containing 10% fetal bovine serum (Avantor), 1% penicillin/streptomycin/amphotericin B (Quality Biological), 1% minimum essential medium (MEM) vitamin solution (Sigma-Aldrich), and 1% MEM nonessential amino acids (Gibco). Cells were blocked for 10 min on ice with anti-mouse CD16/CD32 Fc block (BD Biosciences) in sterile PBS containing 2% bovine serum albumin (Sigma-Aldrich). Following blocking, cells were stained with antibodies specific to CD45 (PE), CD3 (BV510), CD4 (BUV395), CD8a (AF700), CD19 (AF594), CD11c (BV421), MHC class II (I-A/I-E) (BV711), B220 (BV570), and F4/80 (PE/Cy7). Flow cytometry was performed on a BD FACS LSR II. Stopping gates were defined using forward scatter area versus height, forward scatter area versus side scatter area, and positive CD45 fluorescence; 100,000 stopping gate events were collected when possible. Data were subsequently analyzed by using FlowJo v10.

Cytokine Measurement. MLN lymphocytes were plated at a density of 1×10^6 cells in the previously described RPMI 1640 medium with 2 μg of anti-CD3 and 4 μg of anti-CD28. Cells were incubated for 72 h before supernatant collection. Measurement of IL-22 and IL-23 was performed by ELISA (Quantikine) per the manufacturer's instructions.

qRT-PCR. Total RNA was isolated from homogenized colonic tissue using the Aurum total RNA mini kit (Bio-Rad). cDNA was synthesized from 1 μg of total RNA using the iScript cDNA synthesis kit (Bio-Rad). Relative gene expression was determined using the TaqMan method (iTaq Bio-Rad) and appropriate gene-specific primers and probes. Gene expression was normalized to glucuronidase beta (*gusb*) and compared using the ΔΔCt method. The following primers were used in this study: *gusb* (forward: ATGGGATTCATGTGGTGGAAC; reverse: GTTGATGGCAATCGTGATCCG; probe: CCAGAGTGGGCCCCTGACCA) and *Itbr* (forward: ATTGAGCCTCGGACACAAGG; reverse: TGAGCACCACAAAGCTTTGC; probe: TGGTCCCAGGGTCACTCGCA).

GeoMx Whole-Transcriptome Atlas. Four-micron–thick formalin-fixed paraffin-embedded tissue sections were deparaffinized and washed before antigen retrieval in Tris-EDTA (ethylenediaminetetraacetic acid) (pH 9.0; eBioscience). RNA targets were then exposed using Proteinase K (Thermo Fisher) and post-fixed in 10% neutral buffered formalin. Slides were then incubated with GeoMx whole-transcriptome atlas probes at 37 °C overnight in a hybridization chamber (Boekel Scientific). Stringent washes in saline-sodium citrate SSC (Sigma-Aldrich) and 100% deionized formamide (VWR) were performed to remove off-target probes. The slides were then stained with fluorescently labeled morphology markers, including PanCK (AF488; 1:400; Novus), Syto83 nuclear stain (1:25; Invitrogen), anti-alpha smooth muscle actin (AF594; 1:200; Abcam), and CD45 (AF647; 1:100; Cell Signaling Technologies). Slides were then loaded into the GeoMx platform for imaging and barcode acquisition following the manufacturer's instructions. TLOs were identified and marked as regions of interest for barcode acquisition. Library preparation was performed using manufacturer-supplied PCR master mix and well-specified indices to index and amplify the collected regions of interest. Barcodes were then pooled and purified using AMPure XP beads and ethanol washes. A Bioanalyzer DNA high-sensitivity trace was used to assess library quality. Samples were sequenced on an Illumina platform.

Data Analysis. Data are presented as mean ± SEM. Ordinary one-way ANOVA and unpaired Student's *t* tests were used to analyze parametric data. Kruskal–Wallis and Mann–Whitney tests were used for nonparametric analyses. To increase statistical transparency, individual data points are shown, and exact *P* values are reported, with a *P* value of <0.05 considered statistically significant. Cell deconvolution was performed as previously described (26). GraphPad v9.0 and R v4.0 were used to conduct analyses.

Data, Materials, and Software Availability. All study data are included in the article and/or *SI Appendix*. All data is available upon request by the authors.

ACKNOWLEDGMENTS. This work was supported by National Institutes of Health grants DK042191, DK055812, and DK091222 awarded to F.C. and DK122695 awarded to A.G.-N. We also acknowledge the Mouse Models Core and the Histology/Imaging Core of the Cleveland Digestive Disease Research Core Center (DK097948). We also thank Dr. Valeriy Poroyko for his assistance in generating the alluvial plot, Dr. Mohamed Oukka for the IL23r$^{-/-}$ mice, and Natalia Aladyshkina for her management of the mouse colony. Finally, we would like to thank the CWRU Genomics Core Facilities and Cytometry Core Facilities for their assistance with 16S rRNA sequencing and flow cytometry, respectively.

Author affiliations: [a]Digestive Health Research Institute, Case Western Reserve University School of Medicine, Cleveland, OH 44106; [b]Department of Medicine, Case Western Reserve University School of Medicine, Cleveland, OH 44106; and [c]Department of Pathology, Case Western Reserve University School of Medicine, Cleveland, OH 44106

1. H. S. P. de Souza, C. Fiocchi, D. Iliopoulos, The IBD interactome: An integrated view of aetiology, pathogenesis and therapy. *Nat. Rev. Gastroenterol. Hepatol.* **14**, 739–749 (2017).
2. A. Basson, A. Trotter, A. Rodriguez-Palacios, F. Cominelli, Mucosal interactions between genetics, diet, and microbiome in inflammatory bowel disease. *Front. Immunol.* **7**, 290 (2016).
3. J.-F. Colombel, Targeting the preclinical phase of inflammatory bowel disease. *Gastroenterol. Hepatol. (N. Y.)* **11**, 711–713 (2015).
4. D. J. Gracie, E. A. Guthrie, P. J. Hamlin, A. C. Ford, Bi-directionality of brain-gut interactions in patients with inflammatory bowel disease. *Gastroenterology* **154**, 1635–1646 (2018).

5. D. J. Gracie *et al.*, Negative effects on psychological health and quality of life of genuine irritable bowel syndrome-type symptoms in patients with inflammatory bowel disease. *Clin. Gastroenterol. Hepatol.* **15**, 376–384 (2017).
6. C. N. Bernstein *et al.*, A prospective population-based study of triggers of symptomatic flares in IBD. *Am. J. Gastroenterol.* **105**, 1994–2002 (2010).
7. A. Bitton *et al.*, Predicting relapse in Crohn's disease: A biopsychosocial model. *Gut* **57**, 1386–1392 (2008).
8. S. Jaghult *et al.*, Stress as a trigger for relapses in IBD: A case-crossover study. *Gastroenterol. Res.* **6**, 10–16 (2013).
9. X. Gao *et al.*, Chronic stress promotes colitis by disturbing the gut microbiota and triggering immune system response. *Proc. Natl. Acad. Sci. U.S.A.* **115**, E2960–E2969 (2018).
10. S. Melgar, K. Engström, A. Jägervall, V. Martinez, Psychological stress reactivates dextran sulfate sodium-induced chronic colitis in mice. *Stress* **11**, 348–362 (2008).
11. F. Cominelli, K. O. Arseneau, A. Rodriguez-Palacios, T. T. Pizarro, Uncovering pathogenic mechanisms of inflammatory bowel disease using mouse models of Crohn's disease-like ileitis: What is the right model? *Cell. Mol. Gastroenterol. Hepatol.* **4**, 19–32 (2017).
12. R. S. Czepielewski *et al.*, Ileitis-associated tertiary lymphoid organs arise at lymphatic valves and impede mesenteric lymph flow in response to tumor necrosis factor. *Immunity* **54**, 2795–2811 (2021).
13. M. Lochner *et al.*, Microbiota-induced tertiary lymphoid tissues aggravate inflammatory disease in the absence of RORγt and LTi cells. *J. Exp. Med.* **208**, 125–134 (2011).
14. E. N. McNamee, J. Rivera-Nieves, Ectopic tertiary lymphoid tissue in inflammatory bowel disease: Protective or provocateur? *Front. Immunol.* **7**, 308 (2016).
15. Y. Fujimura, R. Kamoi, M. Iida, Pathogenesis of aphthoid ulcers in Crohn's disease: Correlative findings by magnifying colonoscopy, electron microscopy, and immunohistochemistry. *Gut* **38**, 724–732 (1996).
16. M. Buettner, M. Lochner, Development and function of secondary and tertiary lymphoid organs in the small intestine and the colon. *Front. Immunol.* **7**, 342 (2016).
17. A. Vazquez-Tello, R. Halwani, Q. Hamid, S. Al-Muhsen, Glucocorticoid receptor-beta up-regulation and steroid resistance induction by IL-17 and IL-23 cytokine stimulation in peripheral mononuclear cells. *J. Clin. Immunol.* **33**, 466–478 (2013).
18. P. Muller, D. N. Männel, T. Hehlgans, Functional characterization of the mouse lymphotoxin-beta receptor promoter. *Eur. Cytokine Netw.* **12**, 325–330 (2001).
19. R. Ramesh *et al.*, Pro-inflammatory human Th17 cells selectively express P-glycoprotein and are refractory to glucocorticoids. *J. Exp. Med.* **211**, 89–104 (2014).
20. W. Wu *et al.*, Prolactin mediates psychological stress-induced dysfunction of regulatory T cells to facilitate intestinal inflammation. *Gut* **63**, 1883–1892 (2014).
21. T. T. Pizarro *et al.*, SAMP1/YitFc mouse strain: A spontaneous model of Crohn's disease-like ileitis. *Inflamm. Bowel Dis.* **17**, 2566–2584 (2011).
22. A. Gomez-Nguyen *et al.*, Parabacteroides distasonis induces depressive-like behavior in a mouse model of Crohn's disease. *Brain Behav. Immun.* **98**, 245–250 (2021).
23. T. Buynitsky, D. I. Mostofsky, Restraint stress in biobehavioral research: Recent developments. *Neurosci. Biobehav. Rev.* **33**, 1089–1098 (2009).
24. P. H. Thaker *et al.*, Chronic stress promotes tumor growth and angiogenesis in a mouse model of ovarian carcinoma. *Nat. Med.* **12**, 939–944 (2006).
25. A. Rodriguez-Palacios *et al.*, Stereomicroscopic 3D-pattern profiling of murine and human intestinal inflammation reveals unique structural phenotypes. *Nat. Commun.* **6**, 7577 (2015).
26. P. Danaher *et al.*, Advances in mixed cell deconvolution enable quantification of cell types in spatial transcriptomic data. *Nat. Commun.* **13**, 385 (2022).
27. A. D. Kostic, R. J. Xavier, D. Gevers, The microbiome in inflammatory bowel disease: Current status and the future ahead. *Gastroenterology* **146**, 1489–1499 (2014).
28. T. G. Dinan, J. F. Cryan, Gut instincts: Microbiota as a key regulator of brain development, ageing and neurodegeneration. *J. Physiol.* **595**, 489–503 (2017).
29. K. V. Sandhu *et al.*, Feeding the microbiota–gut–brain axis: Diet, microbiome, and neuropsychiatry. *Transl. Res.* **179**, 223–244 (2017).
30. A. Rodriguez-Palacios *et al.*, 'Cyclical Bias' in microbiome research revealed by a portable germ-free housing system using nested isolation. *Sci. Rep.* **8**, 3801 (2018).
31. G. De Palma *et al.*, Transplantation of fecal microbiota from patients with irritable bowel syndrome alters gut function and behavior in recipient mice. *Sci. Transl. Med.* **9**, eaaf6397 (2017).
32. N. Ota *et al.*, IL-22 bridges the lymphotoxin pathway with the maintenance of colonic lymphoid structures during infection with *Citrobacter rodentium*. *Nat. Immunol.* **12**, 941–948 (2011).
33. A. V. Tumanov *et al.*, Lymphotoxin controls the IL-22 protection pathway in gut innate lymphoid cells during mucosal pathogen challenge. *Cell Host Microbe* **10**, 44–53 (2011).
34. M. Keir, Y. Yi, T. Lu, N. Ghilardi, The role of IL-22 in intestinal health and disease. *J. Exp. Med.* **217**, e20192195 (2020).
35. M. E. Mulcahy, J. M. Leech, J.-C. Renauld, K. H. Mills, R. M. McLoughlin, Interleukin-22 regulates antimicrobial peptide expression and keratinocyte differentiation to control *Staphylococcus aureus* colonization of the nasal mucosa. *Mucosal Immunol.* **9**, 1429–1441 (2016).
36. A. Awasthi *et al.*, Cutting edge: IL-23 receptor gfp reporter mice reveal distinct populations of IL-17-producing cells. *J. Immunol.* **182**, 5904–5908 (2009).
37. G. C. Furtado *et al.*, TNFα-dependent development of lymphoid tissue in the absence of RORγt$^+$ lymphoid tissue inducer cells. *Mucosal Immunol.* **7**, 602–614 (2014).
38. T. W. Spahn *et al.*, Induction of colitis in mice deficient of Peyer's patches and mesenteric lymph nodes is associated with increased disease severity and formation of colonic lymphoid patches. *Am. J. Pathol.* **161**, 2273–2282 (2002).
39. F. Barone *et al.*, IL-22 regulates lymphoid chemokine production and assembly of tertiary lymphoid organs. *Proc. Natl. Acad. Sci. U.S.A.* **112**, 11024–11029 (2015).
40. R. Sura, J.-F. Colombel, H. J. Van Kruiningen, Lymphatics, tertiary lymphoid organs and the granulomas of Crohn's disease: An immunohistochemical study. *Aliment. Pharmacol. Ther.* **33**, 930–939 (2011).
41. P. Kiesler, I. J. Fuss, W. Strober, Experimental models of inflammatory bowel diseases. *Cell. Mol. Gastroenterol. Hepatol.* **1**, 154–170 (2015).
42. D. C. Baumgart, W. J. Sandborn, Crohn's disease. *Lancet* **380**, 1590–1605 (2012).
43. B. Boye *et al.*, INSPIRE study: Does stress management improve the course of inflammatory bowel disease and disease-specific quality of life in distressed patients with ulcerative colitis or Crohn's disease? A randomized controlled trial. *Inflamm. Bowel Dis.* **17**, 1863–1873 (2011).
44. B. J. Olivier *et al.*, Vagal innervation is required for the formation of tertiary lymphoid tissue in colitis. *Eur. J. Immunol.* **46**, 2467–2480 (2016).
45. C. Zaph *et al.*, Commensal-dependent expression of IL-25 regulates the IL-23–IL-17 axis in the intestine. *J. Exp. Med.* **205**, 2191–2198 (2008).
46. S. Sawa *et al.*, RORγt$^+$ innate lymphoid cells regulate intestinal homeostasis by integrating negative signals from the symbiotic microbiota. *Nat. Immunol.* **12**, 320–326 (2011).
47. J. S. Johnson *et al.*, Evaluation of 16S rRNA gene sequencing for species and strain-level microbiome analysis. *Nat. Commun.* **10**, 5029 (2019).
48. A. Nakajima *et al.*, IgA regulates the composition and metabolic function of gut microbiota by promoting symbiosis between bacteria. *J. Exp. Med.* **215**, 2019–2034 (2018).
49. T. Rollenske *et al.*, Parallelism of intestinal secretory IgA shapes functional microbial fitness. *Nature* **598**, 657–661 (2021).
50. E. D. Kirby *et al.*, Acute stress enhances adult rat hippocampal neurogenesis and activation of newborn neurons via secreted astrocytic FGF2. *eLife* **2**, e00362 (2013).
51. S. Chetty *et al.*, Stress and glucocorticoids promote oligodendrogenesis in the adult hippocampus. *Mol. Psychiatry* **19**, 1275–1283 (2014).
52. R. W. Stidham, K. Takenaka, Artificial intelligence for disease assessment in inflammatory bowel disease: How will it change our practice? *Gastroenterology* **162**, 1493–1506 (2022).
53. M. Kumar, M. Garand, S. Al Khodor, Integrating omics for a better understanding of inflammatory bowel disease: A step towards personalized medicine. *J. Transl. Med.* **17**, 419 (2019).
54. M. Weiser *et al.*, Molecular classification of Crohn's disease reveals two clinically relevant subtypes. *Gut* **67**, 36–42 (2018).
55. B. Chassaing, J. D. Aitken, M. Malleshappa, M. Vijay-Kumar, Dextran sulfate sodium (DSS)-induced colitis in mice. *Curr. Protoc. Immunol.* **104**, 15.25.1–15.25.14 (2014).
56. J. Gubatan *et al.*, Antimicrobial peptides and the gut microbiome in inflammatory bowel disease. *World J. Gastroenterol.* **27**, 7402–7422 (2021).
57. D. Corridoni *et al.*, Dysregulated NOD2 predisposes SAMP1/YitFc mice to chronic intestinal inflammation. *Proc. Natl. Acad. Sci. U.S.A.* **110**, 16999–17004 (2013).
58. T. Kodani *et al.*, Flexible colonoscopy in mice to evaluate the severity of colitis and colorectal tumors using a validated endoscopic scoring system. *J. Vis. Exp.* 10.3791/50843 (2013).
59. I. Lagkouvardos *et al.*, IMNGS: A comprehensive open resource of processed 16S rRNA microbial profiles for ecology and diversity studies. *Sci. Rep.* **6**, 33721 (2016).
60. I. Lagkouvardos, S. Fischer, N. Kumar, T. Clavel, Rhea: A transparent and modular R pipeline for microbial profiling based on 16S rRNA gene amplicons. *PeerJ* **5**, e2836 (2017).